Phd Thesis

M.C. Orlando Miguel Medina Cázares

July 16, 2014

Contents

List of Figures

Chapter 1

Regularized iterative least-squares algorithm for phase-shifting interferometry

1.1 Introduction

Phase Shifting Interferometry (PSI) demodulation methods are useful 1D temporal linear systems that allow us to recover the modulating phase of the PSI sequence. When the number of samples is small, typically between 3 and 15, we speak of PSI methods [1, 14], but they requiere a constant phase and do not tolerate missing data. On the other hand, when the number of samples is large, between 10^2 and 10^3, we speak of temporal analysis methods [7, 13, 3] which have many problems with the interferogram borders and missing data. Another possibility for analyzing the temporal signal is the use of a running PSI method tuned at the carrier frequency [7, 13, 3, 12, 11, 18]. For example if we use a tree step PSI method we could demodulate the phase locally for each of three consecutive samples. Although this method will deal well with borders, missing data cannot be handled and can even impede the use of this strategy. In experimental methods missing data appear in the case of a saturated signal and also in heterodyne temporal speckle-pattern interferometry when temporal decorrelation appears. Also missing data and discontinuities due to occlusions or shadows are very common in projected fringe profilometry. Besides these problems, noise is another important issue to solve; for example, in speckle techniques [1, 3] noisy interferograms are obtained, in consequence, recovered phase have to be treated to obtain a clean phase easy to unwrap.

Hence, in this paper we are going to present a full-field 2D linear demodulation method that uses in conjunction the temporal and spatial information in order to recover a clean phase, while interpolates empty small sections of missing data from the image space all with low computational time and in the same process.

1.2 Classical Least-Squares

Each (x, y) pixel of the PSI sequence is a 1D temporal discrete interferometric signal modeled in the following way,

$$
\begin{aligned}
I_{x,y}(k) &= a_{x,y} + b_{x,y} \cos(\phi_{x,y} + k\alpha) \\
&= a_{x,y} + c_{x,y} \sin(k\alpha) - s_{x,y} \cos(k\alpha),
\end{aligned} \tag{1.1}
$$

where $c_{x,y} = b_{x,y} \cos(\phi_{x,y})$ and $s_{x,y} = b_{x,y} \sin(\phi_{x,y})$ are the quadrature components of the 1D temporal interferometric signal, k is the discrete temporal variable, $a_{x,y}$ the background illumination, $b_{x,y}$ the modulation term, α the phase step or temporal carrier, and $\phi_{x,y}$ the modulating phase sought at the (x, y) pixel; note that all these variables are scalars. The independent temporal variable k represents the k-frame of the PSI sequence. In this context, knowing the temporal carrier α (phase step as known in PSI), the objective of the PSI demodulation methods is to estimate the quadrature components $c_{x,y}$ and $s_{x,y}$ of the interferometric signal at the (x, y) pixel. Then, the phase at (x, y) is obtained as:

$$
\phi_{x,y} = \arctan\left(\frac{s_{x,y}}{c_{x.y}}\right). \tag{1.2}
$$

Scanning all pixels in this way, we obtain the wrapped phase image of the PSI sequence. One of the first approaches to demodulate a PSI sequence was the least-squares model for PSI [10, 2, 4, 5]. The least-squares model (cost function) for PSI is the following,

$$
U(a_{x,y}, c_{x,y}, s_{x,y}) = \sum_{k=0}^{N-1} [a_{x,y} + c_{x,y} \sin(k\alpha) - s_{x,y} \cos(k\alpha) - I_{x,y}(k)]^2, \tag{1.3}
$$

where $I_{x,y}(k)$ is the observed value of the k-frame at the (x, y) pixel modeled as in Eq. (1.1). To have a well-posed mathematical model for Eq. (1.3), it is necessary to have at least three interferograms in the PSI sequence; that

is, $N \geq 3$. The parameters $c_{x,y}$ and $s_{x,y}$ that minimize Eq. (1.3) are the quadrature components used in Eq. (1.2) to obtain the phase. To minimize Eq. (1.3), we solve a 3×3 linear equation system where $a_{x,y}$, $c_{x,y}$ and $s_{x,y}$ are the unknowns. As the temporal interferometric signal of each pixel has the same model [see Eq. (1.1)], the solution of the linear equation system is always the same. This allows us to demodulate the interferogram sequence using very simple closed mathematical forms [1]. However, as shown in Eq. (1.3), this system never uses the spatial information but the temporal one; in fact, not one of the temporal PSI demodulation methods uses the spatial information [14]. Reason why, using temporal PSI demodulation methods we filter only through the interferogram sequence, but not through the interferogram image space. As a consequence, temporal PSI demodulation methods can not remove unwanted spatial harmonics or noise that may be introduced while recording the interferograms.

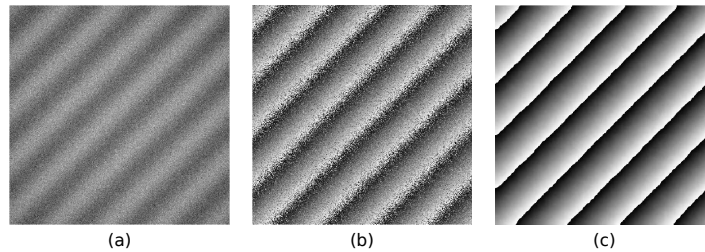

(a)   (b)   (c)

Figure 1.1: Numerical examples. a) One of four simulated interferogram sequences. b) Recovered phase map using classic least-squares. c) Recovered phase map using our proposed *Full-field 2D least-squares*.

1.3 Full-field 2D least-squares method

Regularization systems are very useful full-field systems that can use all the information needed to obtain the data sought as expected. In PSI, we can use these techniques to include the temporal and spatial information to recover the modulating phase as a smooth 2D function, removing unwanted harmonics and noise. Actually, regularization techniques have been used before in PSI for these purposes, the first were Marroquin et al. [7, 8, 9] and more recently others [15, 16, 6, 12, 17, 11, 18]. However, the approach used in those works obtained non-linear systems with a considerable computational work load. Besides, these algorithms need a pre-processing method

to remove background illumination in order to demodulate a correct phase. In our case, this preprocess is not needed and, also and more important, we will maintain the linearity of the least-squares cost function (1.3), adding spatial constraints to recover the wrapped modulating phase while removing noise and unwanted harmonics present in the interferograms [7], besides interpolating small sections of missing data. These constraints will penalize the spatial variations of the quadrature components $c_{x,y}$ and $s_{x,y}$ by using first order potentials as regularization terms. Proceeding in this way, the *Full-field 2D least-squares* cost function for PSI is the following:

$$
\begin{aligned}
U(\mathbf{a}, \mathbf{c}, \mathbf{s}) = \sum_{k=0}^{N-1} \sum_{x,y \in L} & \left[a_{x,y} + c_{x,y} \sin(k\alpha) - s_{x,y} \cos(k\alpha) - I_{x,y}(k) \right]^2 M_{x,y} \\
& + \lambda \sum_{x,y \in L} \left[(c_{x,y} - c_{x-1,y})^2 + (s_{x,y} - s_{x,y-1})^2 \right] \\
& + \mu \sum_{x,y \in L} (a_{x,y} - a_{x-1,y})^2,
\end{aligned}
\tag{1.4}
$$

where $M_{x,y}$ is a binary mask with valid measurement, λ is the regularization parameter that penalizes the spatial variations of quadrature components $\mathbf{c}$ and $\mathbf{s}$, and μ penalizes the spatial variations of background illumination $\mathbf{a}$. Note that in this case, the parameters $(\mathbf{a}, \mathbf{c}, \mathbf{s})$ of the cost function in Eq. (1.4) are scalar fields with dimensions $L_x \times L_y$ and elements $a_{x,y}$, $c_{x,y}$ and $s_{x,y}$, respectively, while the parameters $(a_{x,y}, c_{x,y}, s_{x,y})$ of the cost function in Eq. (1.3) are just scalars. As with the least-squares cost function of Eq. (1.3), here, at least three interferograms are needed in the sequence in oreder to have a well-posed mathematical model. To minimize Eq. (1.4), in order to obtain the quadrature components $\mathbf{c}$ and $\mathbf{s}$ that will give us the modulating phase, we need to solve a linear equation system of $3(L_x \times L_y)$ equations and $3(L_x \times L_y)$ unknowns. Compared with the 3×3 linear equation system of Eq. (1.3), the linear equation system of Eq. (1.4) is larger; however, solving this linear equation system is not so complicated when using numerical methods such as *Gauss-Seidel*. One of the advantages of the *Gauss-Seidel* method is that it is numerically stable, and it is not necessary to build the associated matrix of the linear equation system; besides, the *Gauss-Seidel* method can be programmed for today's modern parallel processors, such as the *Graphics Processing Unit* (GPU), speeding up the minimization process. For illustration purposes, in this paper we programmed the algorithm in *C++* language.
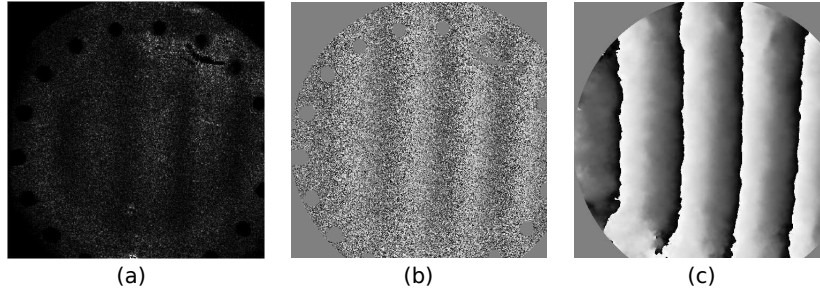
(a) (b) (c)

Figure 1.2: Experimental results. a) One of four experimental interferogram sequences. b) Recovered phase map using classic least-squares. c) Recovered phase map using our proposed *Full-field 2D least-squares*.

1.4 Numerical Experiments

To show the performance of the *Full-field 2D least-squares* algorithm, we simulated a PSI sequence of four interferograms of 512×512 pixels in the following way: $I_{x,y}(k) = a_{x,y} + b_{x,y}cos(\phi_{x,y} + k\alpha) + \eta_{x,y}$, for $k = 0, 1, 2, 3$ and $\alpha = \pi/2$. The modulated phase ϕ was modeled as a plane using the following expression: $\phi_{x,y} = 0.05x + 0.05y$. The background illumination term a was modeled as a parabola centered at pixel $(256,256)$ of the image frames with a dynamic range between 0 and 1. The b term was set to 1. Last, we added a random field of white noise η, with mean $\gamma = 0$ and variance $\sigma^2 = 1$. In Fig. 1.1(a), we see the first interferogram of the simulated sequence. Figures 1.1(b) and 1.1(c) show the wrapped phase using classic least-squares [2] and the *Full-field 2D least-squares* method, respectively. To estimate the wrapped phase in Fig. 1.1(c), we solve the linear system in Eq. (1.4) using the Gauss-Seidel method and setting λ and μ to 50. The number of iterations was 500. For this example, the mask $M_{x,x}$ in Eq. (1.4) is one over all the image; since all the image it is valid information. Computational time was 4.6934 seconds, on a PC with an Intel Core i7 processor and 8 GB RAM memory . We can see in these figures that our proposed method recovers a phase with much less noise than the classic least-squares method, given the regularization terms in Eq. (1.4).

1.5   Experimental Results

Now, we are going to show the performance of our method with experimentally obtained interferograms and compare it qualitatively with the classical least-squares method. The interferogram sequence was generated using an ESPI technique, and the wave-front under test was modified applying pressure. For the phase step, a phase-shift of $\pi/2$ radians was introduced. The object under test was a circular metal plate with circular perforations all along its edge. In order to increase reflexion, we coated the plate with white powder, except for a small part, as can be seen in Fig. 1.2(a). Fig. 1.2(a) shows the first experimental phase-shifting interferogram of a 4 samples sequence. In Fig. 1.2(b), we show the wavefront estimation of the classic least-squares method, while in Fig. 1.2(c), we see the wave-front estimation of the *Full-field 2D least-squares* method proposed here. Computational time in this case was 7.6483 seconds using the PC described above. As we can see, the proposed method was able to estimate a phase free of noise. Another significant feature of this algorithm is that in sections where there is no information, such as black circles and scratches, the algorithm was able to fill-up the empty spaces satisfactorily; this is because it takes into account the neighboring pixel information and the regularization terms; very useful feature in the aforementioned cases.

1.6   Comments and conclusions

The calculation of a free-noise phase in PSI is very useful, since it allows us to use simple algorithms to unwrap the phase. Normally, to get a soft phase, we need to filter the interferogram samples or the output phase to remove the noise. The problem of this process is that we may be removing important information during the filtering. For this reason, the *Full-field 2D least-squares* algorithm represents a significant improvement to the classical least-squares method. Besides, as we have seen before, the presented algorithm is capable of interpolating small empty spaces of missing data, since it takes into account the temporal and spatial information. Therefore, all results presented in this paper can be directly applied to the spatial case where missing data and discontinuities are present. Examples of this are occlusions or shadows in projected fringe profilometry, temporal decorrelation and saturated signal in heterodyne temporal speckle-pattern interferometry.

   Previous to this work, all phase-shifting algorithms only use a single pixel signal to estimate the wave-front under test, regardless of adjacent

information. This paper presents the usefulness of taking into account the temporal and spatial information in conjunction to estimate a best phase map. It is important to highlight that the functional of Eq. (1.4) is a linear system; therefore, it is stable and easy to compute. In conclusion, we present a full-field 2D linear demodulation algorithm able to recover a clean phase and also able to interpolate small empty sections of information, all with low computational time and in the same process.

Bibliography

[1] M. Servin D. Malacara and Z. Malacara. *Interferogram Analysis for Optical Testing*. Taylor & Francis, 2005.

[2] J. E. Greivenkamp. Generalized data reduction for heterodyne interferometry. *Optical Engineering*, 23(4):234350–234350–, 1984.

[3] Pascal Haible, Mahenda P. Kothiyal, and Hans J. Tiziani. Heterodyne temporal speckle-pattern interferometry. *Appl. Opt.*, 39(1):114–117, Jan 2000.

[4] A. Sato K. Okada and J. Tsujiuchi. Simultaneous calculation of phase distribution and scanning phase shift in phase shifting interferometry. *Opt. Commun.*, 84:118–124, 1991.

[5] In-Bok Kong and Seung-Woo Kim. General algorithm of phase-shifting interferometry by iterative least-squares fitting. *Optical Engineering*, 34(1):183–188, 1995.

[6] Ricardo Legarda-Saenz and Mariano Rivera. Fast half-quadratic regularized phase tracking for nonnormalized fringe patterns. *J. Opt. Soc. Am. A*, 23(11):2724–2731, Nov 2006.

[7] J. L. Marroquin, J. E. Figueroa, and M. Servin. Robust quadrature filters. *J. Opt. Soc. Am. A*, 14(4):779–791, Apr 1997.

[8] J. L. Marroquin, M. Servin, and R. Rodriguez-Vera. Adaptive quadrature filters and the recovery of phase from fringe pattern images. *J. Opt. Soc. Am. A*, 14(8):1742–1753, Aug 1997.

[9] J. L. Marroquin, M. Servin, and R. Rodriguez Vera. Adaptive quadrature filters for multiple phase-stepping images. *Opt. Lett.*, 23(4):238–240, Feb 1998.

[10] C. J. Morgan. Least-squares estimation in phase-measurement interferometry. *Opt. Lett.*, 7(8):368–370, Aug 1982.

[11] Julio C. Estrada Orlando Medina and Manuel Servin. Regularized self-tuning phase demodulation for phase-shifting interferometry with arbitrary phase shifts. *Proc. SPIE 8493, Interferometry XVI*, Sep 2012.

[12] Mariano Rivera, Rocky Bizuet, Amalia Martinez, and Juan A. Rayas. Half-quadratic cost function for computing arbitrary phase shifts and phase: Adaptive out of step phase shifting. *Opt. Express*, 14(8):3204–3213, Apr 2006.

[13] Pablo D. Ruiz, Jonathan M. Huntley, and Guillermo H. Kaufmann. Adaptive phase-shifting algorithm for temporal phase evaluation. *J. Opt. Soc. Am. A*, 20(2):325–332, Feb 2003.

[14] M. Servin, J. C. Estrada, and J. A. Quiroga. The general theory of phase shifting algorithms. *Opt. Express*, 17(24):21867–21881, Nov 2009.

[15] M. Servin, J. L. Marroquin, and F. J. Cuevas. Fringe-follower regularized phase tracker for demodulation of closed-fringe interferograms. *J. Opt. Soc. Am. A*, 18(3):689–695, Mar 2001.

[16] Manuel Servin, Jose Luis Marroquin, and Juan Antonio Quiroga. Regularized quadrature and phase tracking from a single closed-fringe interferogram. *J. Opt. Soc. Am. A*, 21(3):411–419, Mar 2004.

[17] J. Vargas, J. Antonio Quiroga, C. O. S. Sorzano, J. C. Estrada, and J. M. Carazo. Two-step interferometry by a regularized optical flow algorithm. *Opt. Lett.*, 36(17):3485–3487, Sep 2011.

[18] Fa Zeng, Qiaofeng Tan, Huarong Gu, and Guofan Jin. Phase extraction from interferograms with unknown tilt phase shifts based on a regularized optical flow method. *Opt. Express*, 21(14):17234–17248, Jul 2013.